Adsorption and experiment design for the environmentally friendly manufacture of copper oxide nanoparticles from olive leaf extraction

Farah S. Daabool | College of biotechnology, Al-Qasim Green University, Hilla, Iraq
Email: farah_s_daabool@uoqasim.edu.iq

ABSTRACT

The creation of CuO nanoparticles have been used olive leaf extraction is focus of the work. Scanning electron microscopy (SEM) revealed that the green-produced copper oxide nanoparticles were spherical, with a mean particle size of 74 nm. CuO nanoparticles were seen in their crystalline and monoclinic phases on the XRD graph. The Debye-Scherrer formula showed that 80 nm was the average crystal size. Using crystal violet, the nano-adsorbents' adsorption properties were investigated, and the adsorption performance at room temperature was 87 mg/g. At pH 4, crystal violet dye is most successfully adsorb able by CuO NPs, Upon adding the CV in concentrations of 0.06 g/0.05 L. Absorption was utilized to optimize a number of process variables, including pH solution (X1: 2 - 11), adsorbing dose (X2: 0.01 - 0.08 g/L), and [CV] dye concentration (X3: 10 - 80 mg/L). The chosen Response surface methodology (RSM) was successful in optimizing the decolorization conditions of CV, as shown by the adjusted coefficient of determination (R2) value of 0.99, which also showed that the utilized model was highly appropriate.

Keywords: | CuO Nanoparticles, Removal dye, Crystal violet , Green synthesis, Response surface methodology.

1.Introduction

An azo dye called Crystal Violet (CV) is employed in the textile, food, paper, and leather sectors. However, there are significant environmental issues brought on by the release of CV and its derivatives into the environment (1).

Without a doubt, adsorption is a straightforward, affordable, efficient, dependable, and often employed separation technique in the treatment of contaminated water. This technique has been proven to be effective at getting rid of aqueous pollutants for a number of years. The complete removal of different hues from water streams by nanoparticles acting as adsorbents has made water purification possible. An acidic and basic dyes' adsorption can be improved by using very nanoscale adsorbents (2).

With fewer experiments, it is simple, effective, and economical to optimize a variety of parameters using the response surface method (RSM). Two other benefits are the ability to specify the optimal theoretical circumstances and do variational analysis to get the final equation for elimination.

This approach can be applied in the form of using the Box-Behnken method (3). There are many experimental designs that have been proven to be efficient for optimizing the process parameters. When large obstacles obstruct optimization, Application of response surface methodology (RSM). Of all RSM designs, Using the Box-Behnken design optimize a four-

factor process with the least amount of experience and is employed to prevent trials carried out in extreme situations.

Although there are many different kinds metal oxide nanoparticles, namely copper oxide nanoparticles. are of particular interest due to their potential for usage in both scientific and commercial endeavors (4).

Given that they are similar to more metallic nanoparticles and have exceptional photocatalytic activity (5). The manufacturing of copper oxide has piqued researchers' interest due to its vast range of applications (6). A semi-conductive substance having a wide range of electrical, optical, and magnetic characteristics is copper oxide. Little study has also been done on the use of copper oxide nanoparticles as adsorbents for color removal. CuO nanoparticles (CuO NPs) do, in fact, have a smaller diffusion channel than more traditional adsorbents like activated carbon, which leads to a larger adsorption capacity and quicker kinetics. As a result, Environmental contaminants may be successfully removed by nano-CuO, it has been found.

Numerous investigations on metal oxide-dependent nanoparticles in nanoscale adsorbents have been done during the past 10 years. Numerous techniques, such as precipitation and co-precipitation (7), have been used to produce CuO nanoparticles, thermal decomposition (8), and sol-gel (9).

In the modern era, green synthesis is crucial for production of CuO nanoparticlesIt gets rid of the hazardous compounds produced by chemical operations as well as the organic solvent utilized in synthetic treatments. Plant extracts have the benefit of offering a biological synthesis method that is less expensive, harmless, and welcoming, and allows for a controlled synthesis with predetermined nanoparticle size and shape(10).

Recently, plant-based nanoparticle synthesis has become more well-liked as a low-cost, ecologically acceptable substitute for physical and chemical techniques. In this industry, a wide range of plants have been investigated for their capacity to produce copper oxide nanoparticles. Here are a few instances of plant extracts: Banana peel extract, Drypetes sepiaria leaf extract, Nerium oleander leaves extract, Ruellia tuberosa leaf extract (11), Nerium oleander leaf extract (12), and Aloe.

We made CuO NPs using olives as a stabilizer, leaf extract, and we demonstrated in this study that they had the capacity to remove the water color CV. Here, first time a straightforward and green invention approach for creating CuO nanoparticles using aqueous leaf extract is provided. We also looked at how well biosynthesised CuO nanoparticles removed the organic dye CV from polluted water(13).

CuO is frequently used as an adsorbent to remove CV from aqueous solutions, Developing is the key objective. approaches evaluating CV adsorption capabilities this material. Then an analysis using the Box-Behnken design is performed the effects of pH, adsorbent dose, and dye concentration on the adsorption system. The research also sought to determine how the factors taken into consideration interacted with one another as well as the optimal operational conditions under which the procedure should be performed(14). As a result, much fewer tests are required. Its key benefit is the potential for the process industries' ability to save time and money. The objective of this research is to evaluate and comprehend the possibility of using CuO NPs generated as an adsorption to reduce.

2.Materials and methods
2.1. Chemicals and materials
Sigma Aldrich supplied anhydrous CuSO4 with purity 95%. (C16H18N3SCl, molecular weight(M.Wt) = 319.85 g/mol, maximum wavelength(λ) = 464 nm) CV from Sigma Aldrich. The extract and the metal salt solutions were made with distilled water.

2.2. Making leaf extract
In a 250 mL beaker, 100 g of fresh leaves of olive were combined with 250 mL of D. W. and cooked at 65 °C for 60 minutes. By centrifuging the light yellow extract produced by the separation of the leaf debris for ten minutes at a speed of 10,000 rpm, a fresh supernatant was obtained for the creation of nanoparticles.

2.3. Protocol for biosynthesis is described.
The produced leaf extract was mixed in a 3:7 proportion Using an anhydrous $CuSO_4$ solution of 1 mM concentration. to produce CuO NPs

(Fig. 1). For two hours, At 25 °C, the mixture was incorporated. The brown tint of the solution indicates the production of CuO NPs. The colloidal was incubated for 24 hours before being centrifuged for 10 minutes producing a pellet at 10,000 rpm. After that, the pellet was cleaned by being rinsed three to five times in double-distilled water. The completed product was collected, processed, and stored for later use after being calcined at 400 °C in an insulated furnace to remove the associated plant organic matter.

2.4. Characterization of created nanoparticles.

The first indication that Cu ions had been bioreduced to molecules of CuO NPs was a noticeable change in hue. The produced structure of the nanoparticles was ascertained by scanning the dry powder using XRD possessing a dispersion angle (2) from 15 to 70. Dryed, mixed with KBr, and subjected to FTIR measurement between 400 and 4000 cm1, the centrifuged nanoparticle pellet was then examined. These biomolecules were found using this spectrum to reduce, cap, and stabilize the nanoparticles that were created.

2.5. studying adsorption

Studies on group adsorption have been carried out to determine the dye's capacity for adsorption. Investigated were a dye's initial concentration's (10 to 80 ppm) effects, adsorbent dose (1 to 8 g/1000ml), and time contact from 20 minute to 6 hours. While examining The values of the other variables remained constant for each parameter alone.. First, 50 mL of the dye solution was mixed with known quantities of the as-synthesised CuO NPs. The mixture was then given a 300 rpm magnetic stirrer agitation at room temperature. The samples were collected at various predetermined intervals, centrifuged at 10,000 rpm for 15 minutes, and the amount of CV dye in each sample was then quantified. An analysis of the outcomes was then performed using the use of a 592 nm ultraviolet-visible spectrophotometer.

Using fluctuations in CV concentration during the aqueous media adsorption , as given in Eq. (1), the amount of adsorbent was calculated.

$$qe = \frac{(C0 - Cf) * V}{m} \tag{1}$$

Where C0 and Cf are the initial and ultimate (equilibrium) concentrations of CV (in milligrams per liter, respectively). The weight of the adsorbent employed is m, and V is the volume of the CV solution (L). Using the equation Eq (2) below, we can get the rate of color removal:

$$CV\ removel\ \% = \frac{Ci - Ce}{Ci} * 100 \tag{2}$$

We will assess the effects of several important parameters on adsorption, including pH, CuO concentration, starting dye concentration, contact duration, salt mass, and temperature.

2.6. Box-Behnken design

A statistical and mathematical method is called "response surface methodology" (RSM) that identifies the ideal circumstances for conducting tests with the least amount of anticipated experiments (15). In order to maximize the answer, it was also employed as an empirical study to look into the connection between the total number of independent factors and the results of the measurements. The Box-Behnken design (BBD) was used to show how the independent variables related to the response function. Utilizing Minitab-17 software, the CV removal procedure on CuO NPs was A Box Behnken design containing three elements, a total of three levels (-1, 0 and + 1), and fifteen runs of experiments was used to optimize the system.

There are three independent variables: initial CV concentration, dosage, and pH (X1, X2, X3) were chosen to examine if certain factors had a significant effect on the adsorption process. The predicted response derived from the model, analysis of variance (ANOVA), and polynomial equation applied to experimental data were utilized to evaluate the outcomes. The study's design goal was to maximize the experimental conditions in order to get the best CV elimination by CuO. Table 1 lists the method parameters and their values based on the results of the preliminary testing. The surface response model was utilized to assess the experimental data, and Eq. (3) was used to estimate the second-order polynomial model.

$$Y = b0 + \sum bjXj + \sum bjjXj2 + \sum bijXiXj \qquad (3)$$

Where Y (% dye removal) stands for the experimental result, Xi is the code variable, b0 is a constant, bj, bjj stand for the coefficients of the linear and quadratic effects, respectively, and bij stands for the contraction coefficient between factor i and j. Xi and Xj are code predicted values for the independent factors. Equation (3) represents the relationship between the crucial factors X1, X2, and X3, as well as the response (Y).

ANOVA, statistical analysis that includes the coefficient of determination (R2), and the performance of the second-order polynomial equation, and Fischer's test (F-test), which measures statistical significance, was used to determine whether it was effective. The accuracy of the model was evaluated using the coefficient of determination (R2). The response's surface and contour plots were put to the test. The contour and surface plots clearly showed the relationship between the important components. The statistical program Minitab v.17 was used for the RSM, ANOVA, and optimization processes.

Table 1. coded levels of factors evaluated using Box –Behnken (BB) design

	pH	Mass(g)	[CV] (ppm)
Low (-1)	2	0.01	10
Center(0)	6.5	0.045	45
High(+1)	11	0.08	80

2.7. Parameters for the Langmuir, Freundlich, and Temkin models

Three models were employed in this work to examine the relationship between the equilibrium CV concentration and the amount of CV adsorbed. Application of the isotherm models to the experimental circumstances of adsorption study (concentration 10-80 ppm , amount of adsorbent 4 g/l, temp 25 °C, and contact period 2 h) was assessed using the coefficient of correlation R2 value for each plot. The fit was enhanced by a higher R2 value. The Freundlich, Temkin, and Langmuir equilibrium isotherm models were fitted to the adsorption data in this investigation, and the corresponding correlation coefficients (R2) for each model were determined.

The idealized presumption of equal thermal and monolayer absorption underlies the isotherm of Langmuir model (16).

$$q_e = \frac{q_m b C_e}{(1+b C_e)}$$

In this equation, Ce (ppm) concentration of CV, qe (mg/g) amount of dyes adsorbed, qm (Langmuir constants) for the monolayer capacity for adsorption and b affinity of the adsorbent towards the adsorbate.

The adsorption results plot and the plot of qe versus Ce, were used to establish the Langmuir constants (Table 3). The significant RL factor, which was determined for all dye concentrations, showed that the entire process was excellent because its values fell within the range of 0 RL 1. The RL equation, as mentioned by

$$R_L = \frac{1}{(1+bC_0)}$$

Where C0 (mg/L) is the dye's starting concentration and b is the Langmuir constant. According to the Freundlich model (17), adsorbate molecules will form. Multilayers have developed on the surface of the adsorbent as a result of the numerous sites of action on the outermost layer having different affinities. The following is the non-linear version of the Freundlich model:

$$q_e = K_F C_e^{1/n}$$

where KF and n are the Freundlich equilibrium coefficients, Ce (ppm) is the equilibrium concentration of the adsorbate, qe (mg/g) is

the amount of dye adsorbed at equilibrium, and q_e (mg/g) is the equilibrium amount of dye. The term KF stands for the adsorbate's adsorption capacity, while the number of n represents how advantageous the adsorption process is When q_e was plotted vs C_e, unsatisfactory curves were produced, demonstrating that the absorption process did not follow this paradigm. Calculating the Freundlich equilibrium constants KF and n was done using the adsorption data plot (Table 3). The metric 1/n, which has a quantitative value between 0 and 1, gauges the level of surface heterogeneity or adsorption intensity.

The Temkin model, relationships between adsorbent-adsorbate must be taken into account throughout the adsorption process and lead to a linear reduction in adsorption heat with adsorbate coverage. The following is a description of the Temkin model:

$$q_e = Bln(AC_e)$$

Where The amount of CV adsorption at equilibrium is C_e (mg/L), and B (related to the heat of adsorption), Q_e (mg/g) is the experimental adsorption capacity, kT (equal to the equilibrium binding constant) is the equilibrium binding constant indicating the maximum binding energy, and C_e (ppm) is the concentration of dyes adsorbed.

$$B = \frac{RT}{b_T}$$

R is the universal gas constant (8.314 J/mol K), and T is the temperature in Kelvin (K), where $1/bT$ is the adsorption potential of the adsorbent.

As the adsorption sites are loaded, adsorption energy drops linearly, as shown by a q_e vs C_e conflict (Table 3). All molecules in the layer experience a linear drop in heat of adsorption as surface coverage increases due to interactions between the adsorbent and adsorbate. Additionally, it implies that, up to a certain amount, the binding energies in adsorption are distributed uniformly.

2.8.Contact time and kinetic analysis

The second-order and pseudo-first-order models were used to calculate the kinetic parameters.

The following formula is used to explain systems with solids and liquids that adsorb using Lagergren's suggested pseudo-first-order kinetic model:

$$log(q_e - q_t) = log(q_e) - \left(\frac{k_1}{2.303}\right)t$$

where q_t (mg/g) denotes the quantity of dye adsorbed at any given time t (min) and q_e (mg/g) denotes the amount of dye adsorbed at the equilibrium time, respectively, and k_1 (1/min) is the rate constant of the pseudo-first-order adsorption. A plot of log (q_e - q_t) against t is used to determine k_1.

The pseudo-second-order kinetic model can be represented in linear form as:(10(
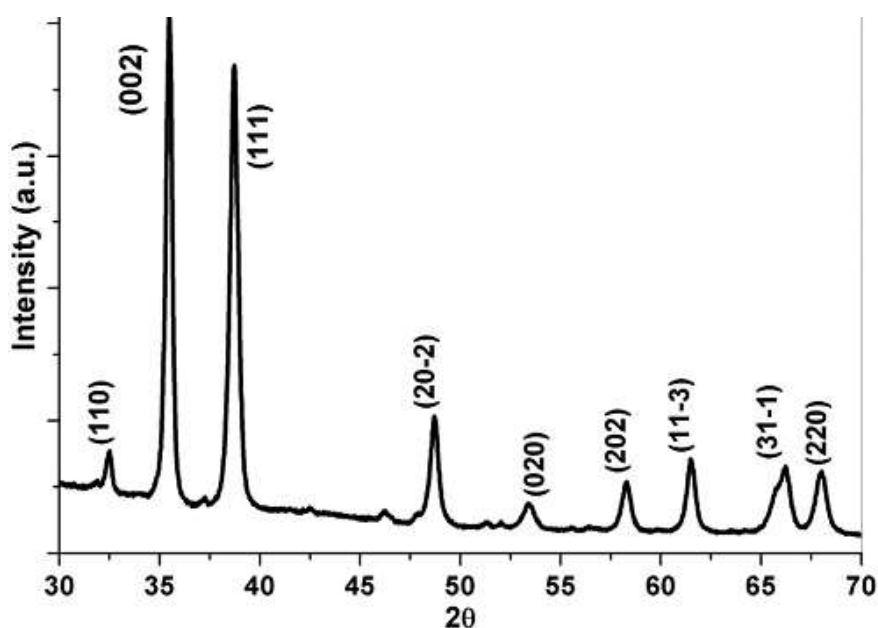
$$\frac{t}{q_t} = \frac{1}{k_2 q_e^2} + \frac{t}{q_e}$$

where k_2 (g/(mg min)) is the pseudo-second-order adsorption rate constant determined using linear t/q_t vs t graphs.

3. Results and analysis

3.1. CuO nanoparticle characterization

CuO Nps formed during biosynthesis were studied using X-ray diffraction (XRD), and the results showed a succession of peaks associated to the monoclinic CuO (1 1 0), (1 1 1), (2 0 2), (0 2 0), (1 1 3), (3 1 1), and (0 0 4) planes. CuO was formed as a result of the

discovery of diffraction peaks (between 2 = 35 and 39°) (18). This demonstrates the expansion of monoclinic crystalline morphology.

According to Bashiri Rezaie et al. (19), XRD patterns show that Copper Oxide nanoparticles are crystalline because they are well-defined and strongly reflected in them. The new findings therefore accord with earlier studies on CuO production (20). The lattice parameters for artificial CuO NPs were a = 4.684, b = 3.425, and c = 5.129. By measuring the peaks' peaks in the XRD spectrum's width, Debye-Scherrer formulas (21) were used to determine the typical size of CuO NPs. Table 2 displays the computed size and peak indexing.

Figure1 : XRD pattern of CuO nanoparticles

Table 2: levels of independent variables used in Box-Behnken design

hkl	2Θ(°)	β(°)	Cos(°)	k	D (nm)
110	32.5	0.00168	2.76	0.92	82.220
002	35.2	0.0033	2.55	0.92	39.111
111	38.9	0.0020	2.39	0.92	68.210
202	48.4	0.0012	1.88	0.92	144.120
020	53.6	0.0017	1.70	0.92	81.110
202	58	0.0035	1.48	0.92	43.111
113	62.5	0.0012	1.42	0.92	144.132
311	66.2	0.0016	1.369	0.92	101.213
220	68.2	0.0019	1.348	0.92	92.321

Table 3: Isotherms parameters for CV adsorption by CuO NPs

Isotherm model	Parameters	
Langmuir	qm(mg/g)	90
	b(ppm)	0.6
	R^2	0.99
Freundlich	N	2
	Kl	29
	R^2	0.8
Temkin	A	4
	B	17.5
	R^2	0.85

It was determined using FTIR analysis if biomolecules from olive extracts may employed to synthesize CuO NPs as well as to characterize the stretching and vibrating modes in biosynthesized materials. The bandwidth in Fig. 2 at 3480 cm1 represents the stretching frequencies of the single bond Copper oxide nanoparticles' surface, there is an OH group from water that has been absorbed. Peaks at 530 cm1 and 580 cm1, which are

ascribed to Cusingle bondO vibrations, offered more proof that CuO nanoparticles had been
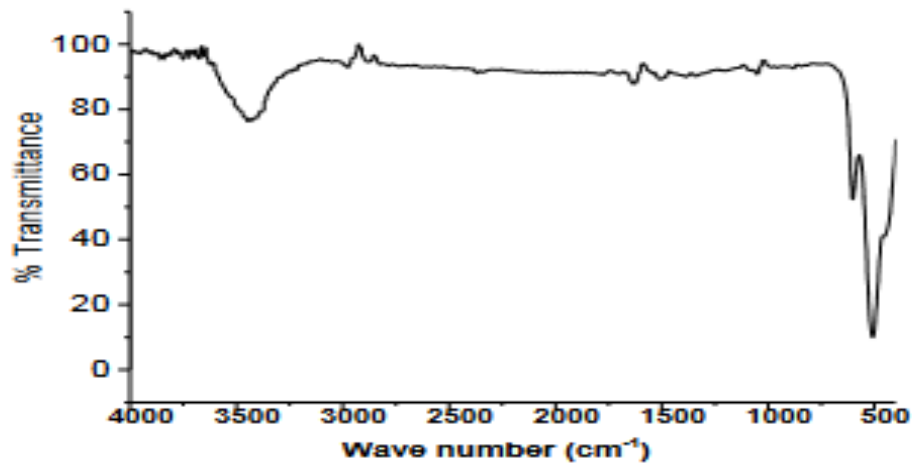
created (22).

Figure 2: FTIR of CuO nanoparticles

SEM was used to assess the morphological characteristics of the produced CuO NPs. The SEM image in Figure 3 depicts the characteristic rod shape of the produced CuO NPs. CuO nanoparticles are made biologically using homogeneous-dimension quasi-spherical particles of relatively tiny size have been found.

The modest aggregation in the as-produced nanoparticles could be attributed to the process of synthesizing things using biological components. The spherical shape of the CuO NPs produced from leaf extract was consistent with earlier discoveries (23).
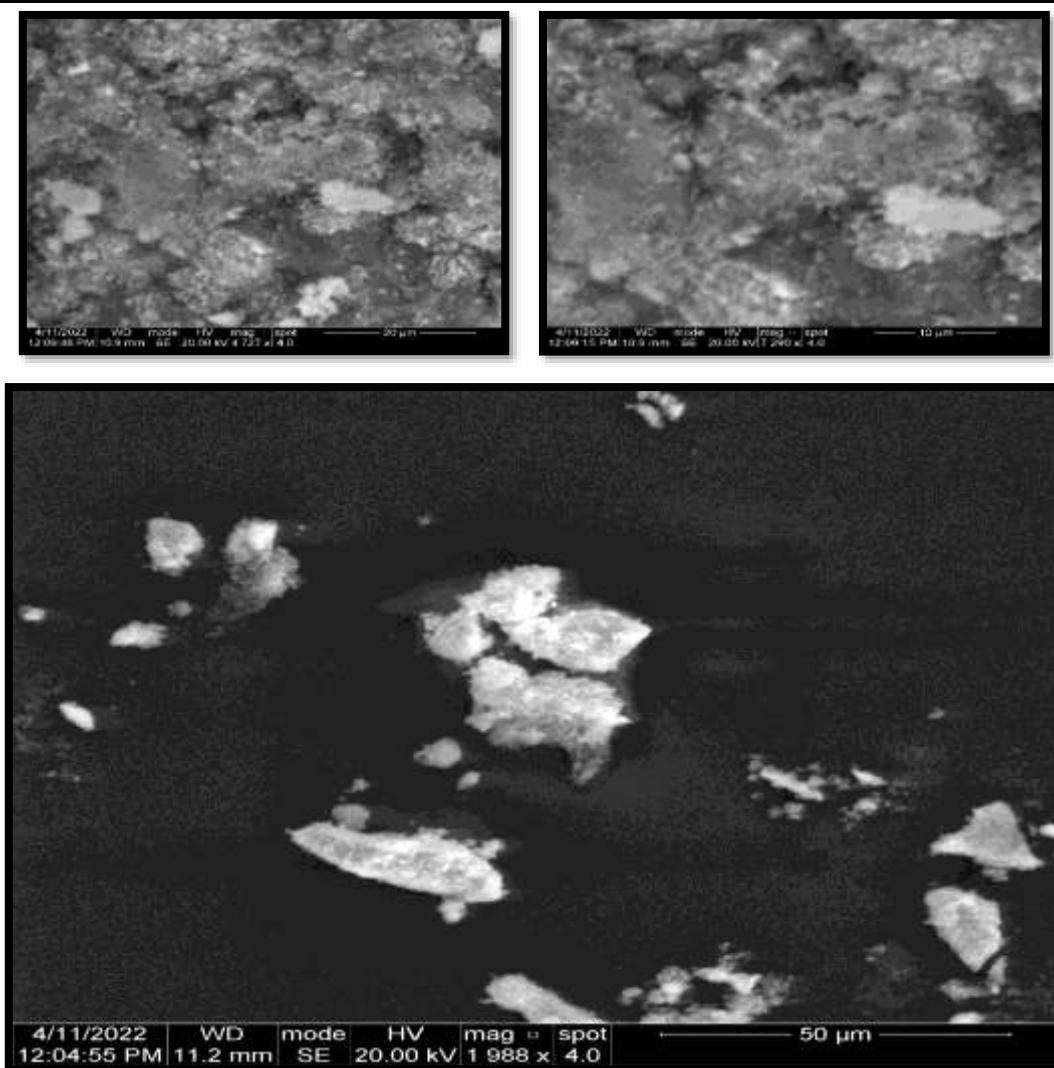
Figure 3: SEM of CuO NPs

3.2. CuO NPs production mechanism

A small number of the biomolecules found in extracts of plants are not required for the creation of nanoparticles, making this procedure easier. from such extracts difficult. Even predicting the precise mechanism of the summary process is difficult. As mentioned earlier, the key functional groups for nanoparticle reduction and stabilization are amine, carbonyl, hydroxyl, and methoxide. Alkaloids, sugars, flavonoids, phenols, and proteins are examples of plant metabolites that include these functional groups (24). The process by which CuO nanoparticles are made may be explained as follows: the polyphenols in olive leaf extract combine with Cu2+ ions to create metal complexes that are then broken down into CuO seed particles. Aggregation occurs to the seed particles before nucleation. Fig. 4 provides a visual representation of the process that creates CuO NPs. Similar manufacturing techniques for nanoparticles have been hypothesized before (25).
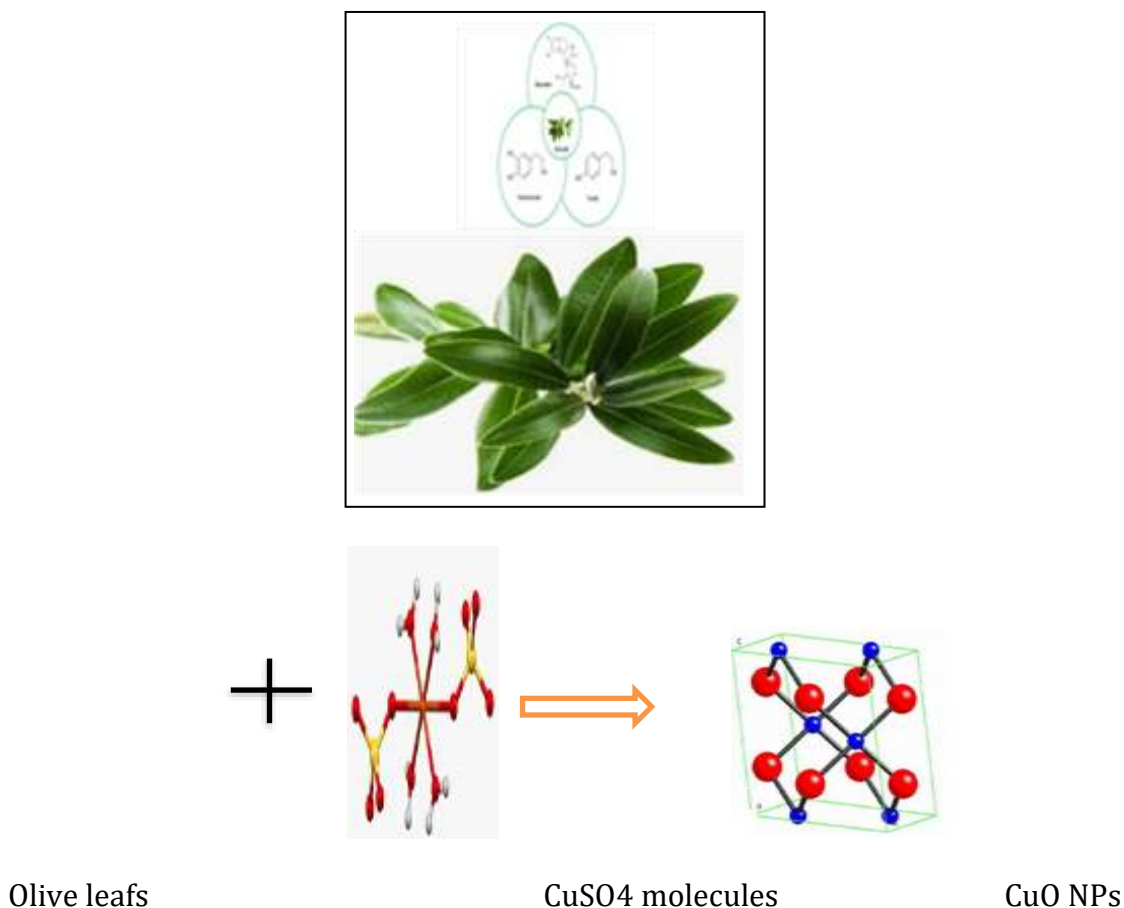
Olive leafs   CuSO4 molecules   CuO NPs
Figure 4: formation of CuO NPs from olive leafs

.

4 Results of Adsorption
4.1. pH Effective

pH significantly affects both the locations where molecules of adsorbents and adsorbates are active during the adsorption process. Fig. 5 illustrates how pH affects dye adsorption onto CuO nanoparticles. The pH range from 2 to 6 saw a rise in dye removal, which subsequently abruptly declined at higher pH values up to 11. With positively charged CuO NPs as active sites, CV molecules generate monovalent ion of nitrogen with a positive charge (H+) at weakly acidic pHs, which results in electrostatic repulsion and lowers the potential quantity of CV that may be adsorbed. The maximum adsorption at pH 6 may be due to functional group CuO NPs protonation. The CV ions and OH- ions are forced to compete with one another for places to adsorb on the copper oxide NPs surface at the pH above 6, which separates that is positive charge, occure precipitate happen. It is likely that a strong Coulomb interaction was established between the positive adsorption active sites of CuO NPs and the deprotonated (negatively charged) CV during the process of CV adsorption. A few research' findings suggest that elevating pH promotes cationic dye adsorption (26). The experiments' findings led to the conclusion that a pH of 6 was the ideal pH level.
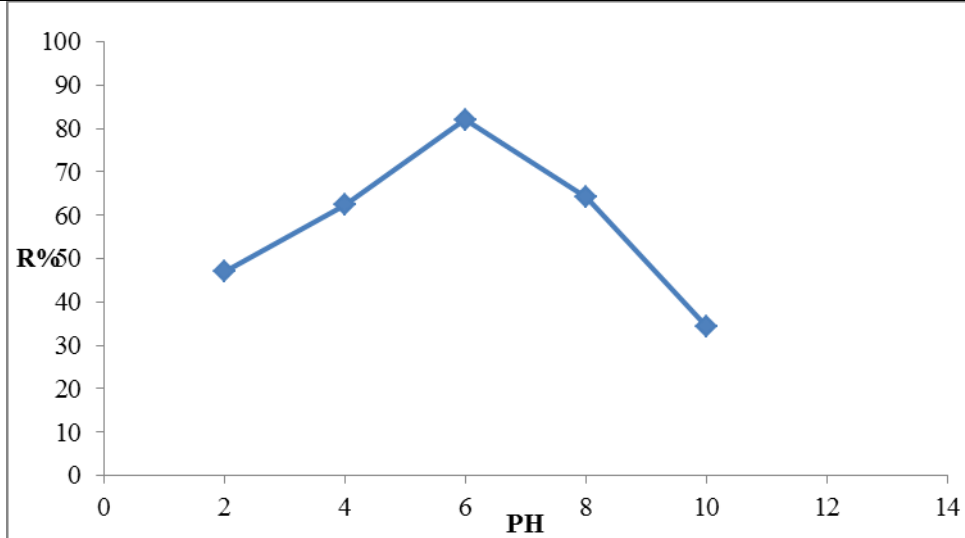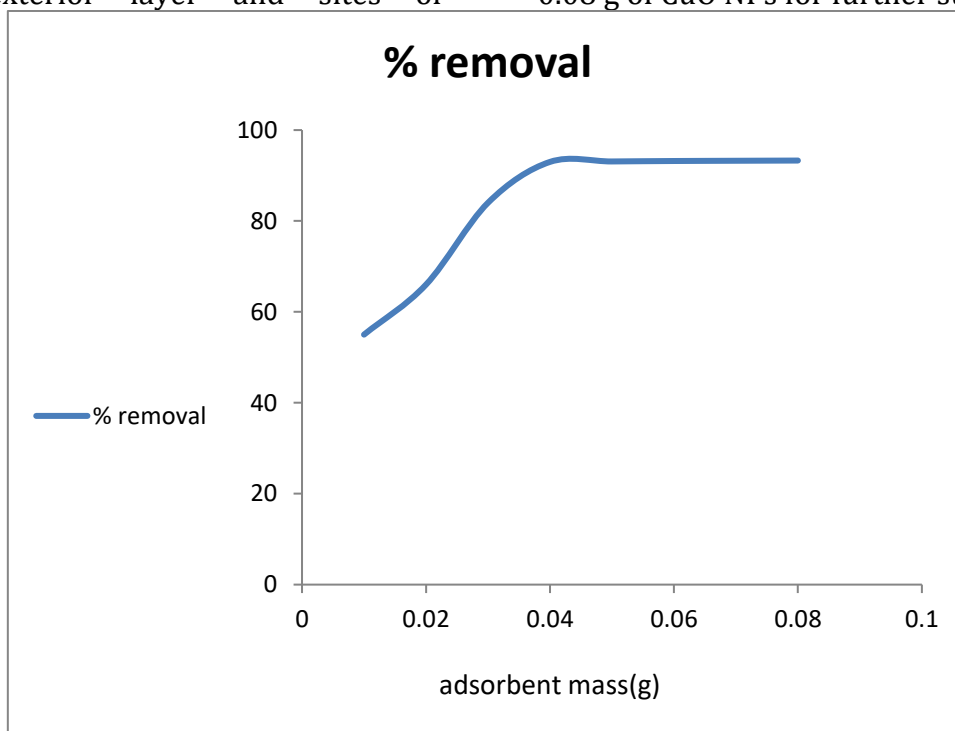
Figure 5: effective of pH on removal of CV dye.

4.2. Mass adsorbent effective

The ideal starting adsorbent dosage is essential because the amount of surface area and the number of binding sites may be limited (1). Fig. 6 depicts the impact of adsorbent dose on CV adsorption. During the first dosage of 0.01-0.08 g, the increase in% CV clearance was rapid. After that, it increased progressively until it reached the equilibrium state of 0.1 g. The adsorbent's exterior layer and sites of adsorption grow when the dosage is raised, enhancing the effectiveness of % removal. The availability of larger surface area is responsible for the enhancement in dye removal (27). The decline in adsorption quantity (qe) at a greater dosage may be attributed to the readily available lower CV molecules since there are more sites that are active on the CuO NPs surface. This experiment led to the selection of 0.08 g of CuO NPs for further study.

Figure 6: effect of adsorbent mass on removal of CV dye.

4.3. Isotherms study and initial concentration effective

The adsorption of CV was investigated using the Langmuir, Freundlich, and Temkin methods (Figs. 7a, 7b, and 7c). Table 3 reports the three

model parameters that were derived. The Langmuir model (R2 > 0.96), which suggests that the monolayer used for CV adsorption, looked more appropriate to represent the experimental data after assessing the correlation coefficient. Using the Freundlich model, the parameter "n" was obtained may also be used to evaluate the favorability of the phenomenon. The sorption of these dye molecules was favorable and moderate, according to data from 1< n< 2.
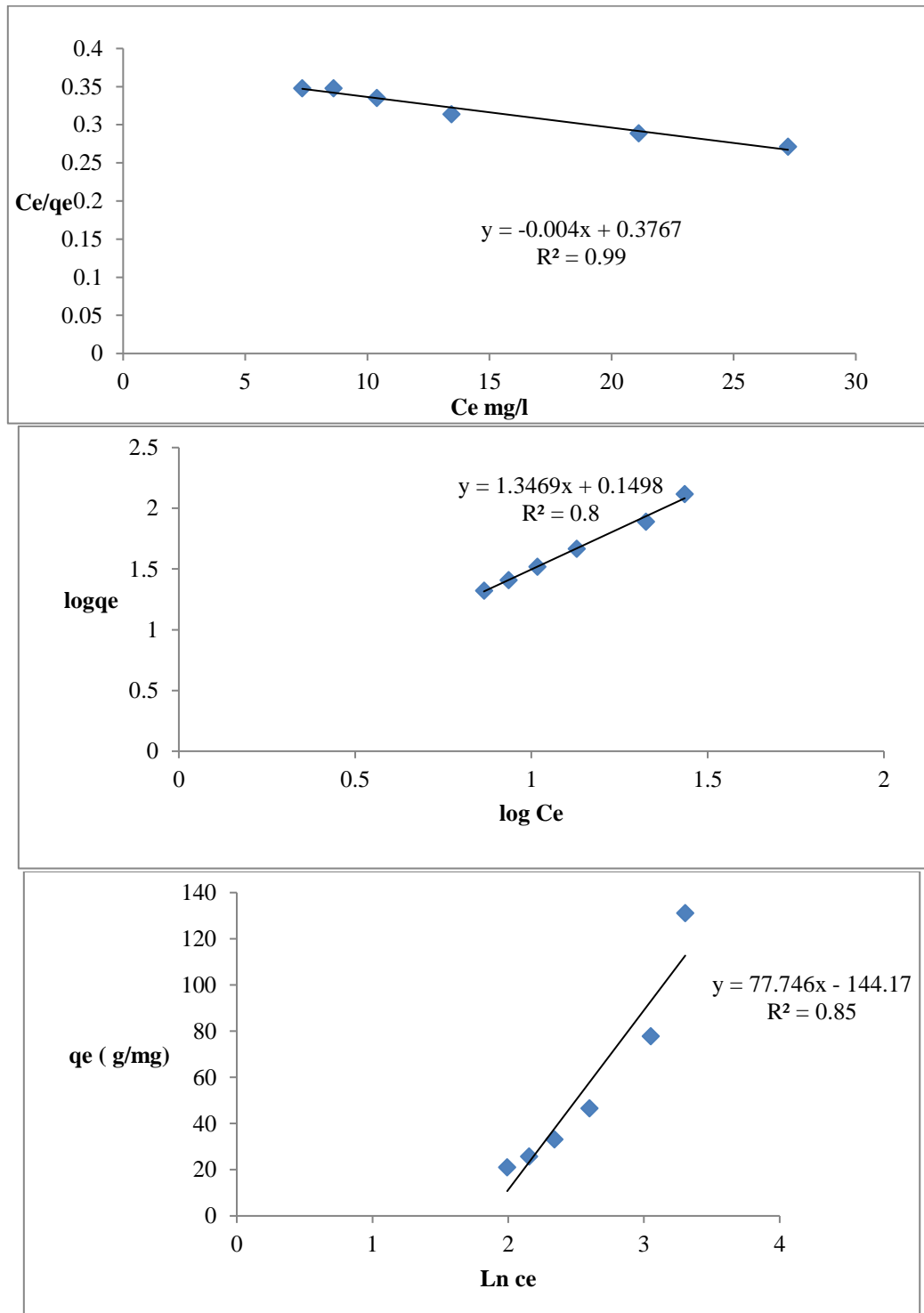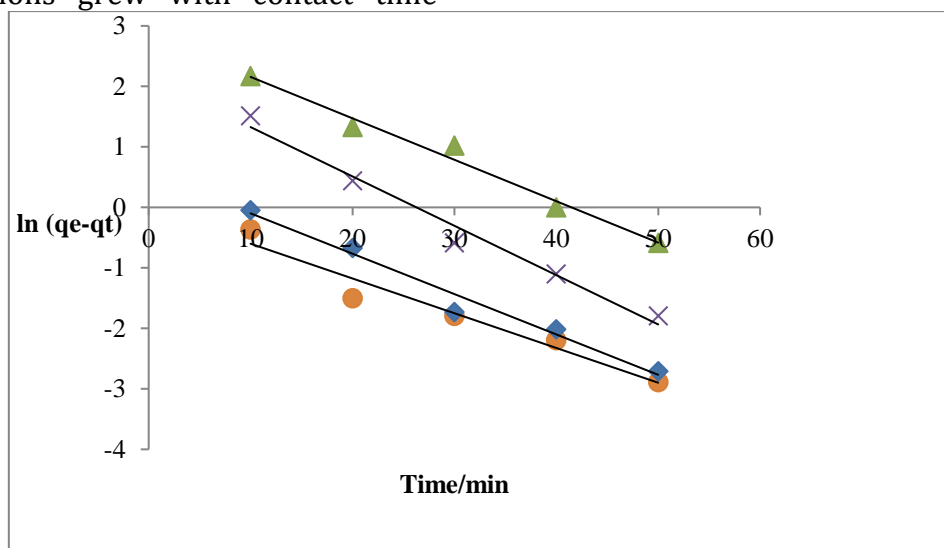

Figure 7: isotherms of adsorption a-Langmiur b- Freundlich c- Temkin

The isotherm profiles of CuO NPs for CV are shown in Fig. 7. The experimental data can be accurately represented by the Langmuir isotherm. The results show that this work is beneficial and effective (28).

4.4. Kinetic study and contact time effective

Fig. 8 shows The pseudo-first order kinetic model adsorption at various from 10 to 80 ppm for initial concentrations. The rate of adsorption rises as the starting concentration does as well. Similar findings were made by (29) decolorations grew with contact time while nanoparticle concentrations remained constant. More contact time gives the response more time to occur. The duration that CuO NPs were incubated also increased the rate of Coomassie's stunning blue coloring (30).

Figure 8: The pseudo-first order kinetic model.

Conclusion

Using a fresh biological extract generated from olive leaf, CuSO4 ions effectively transformed into CuO nanoparticles. The created particles eventually took on a face-centered cubic shape. The earlier research shows the CV was removed from aqueous solutions using CuO nanoparticles. They have a 92,2 mg/g CV adsorption capacity (pH = 6, adsorbent mass = 0.045 g). There have been descriptions of several factors, including adsorbent weight, temperature, and pH. CuO NPs dose of 0.045 g/L, dye concentration of 45 mg/L, and solution pH of 6 were found to be the best experimental conditions for color removal. The experimental results and the Langmuir adsorption isotherm model showed good agreement. However, a pseudo-second-order kinetic model of the CV adsorption on CuO nanoparticles suggests that the adsorption behavior may be controlled by hydrogen bonding between the adsorbent and adsorbate. A Box-Behnken experimental design based on response surface methodology was used to identify the best operational variables in order to improve dye removal efficiency. The experimental data have been well-suited by the model for the best design. This model's p-value was 0.05, indicating that it may be very significant. The ideal conditions for CV removal were determined Using a response surface approach and an experimental design, the following parameters were used: X1 = 6 for the pH X2 = 45 mg/L for the CV quantity, X3 = 4 g/L for the adsorbent mass, and X1 = the solution's concentration level.

References:

1. Abdel-Monem, M., Hegazy, O., Omar, N., Trad, K., Van den Bossche, P., Van Mierlo, J., 2017. Lithium-ion batteries: Comprehensive technical analysis of second-life batteries for smart grid applications. In: 19th European Conference on Power Electronics and Applications (EPE'17 ECCE Europe). https://doi.org/10.23919/epe17ecceeurope.2017.
2. Abo Zeid, E.F., Ibrahem, I.A., Mohamed, W.A.A., Ali, A.M., 2020.Study the influence of silver and cobalt on the photocatalytic activity of copper oxide nanoparticles for the degradation of methyl orange and real wastewater dyes. Mater. Res. Exp. 7,. https://doi.

org/10.1088/2053-1591/ab7400 026201.

3. Ahmad, A., Razali, M.H., Mamat, M., Mehamod, F.S.B., Anuar Mat Amin, K., 2017. Adsorption of methyl orange by synthesized and functionalized-CNTs with 3-aminopropyltriethoxysilane loaded TiO2 nanocomposites. Chemosphere 168, 474–482. https://doi.org/10.1016/j.chemosphere .2016.11.028.

4. Alhalili, Z., Romdhani, C., Chemingui, H., Smiri, M., 2021. Removalof dithioterethiol (DTT) from water by of cellulose acetate (AC) and AC doped ZnO and TiO2 nanoparticles. J. Saudi Chem. Soc. 25, (8). https://doi.org/10.1016/j.jscs.2021.101 282 101282.

5. Amin, F., Baharullah, Khattak F., Alotaibi, A., Qasim, M., Ahmad,I., Ullah, R., Bourhia, M., Saira Zahoor, A.G., Ahmad, R., 2021.Green Synthesis of Copper Oxide Nanoparticles Using Aerva javanica Leaf Extract and Their Characterization and Investigation of In Vitro Antimicrobial Potential and Cytotoxic Activities. Evi. Based Comp. Alt. Med. 2021. https://doi.org/10.1155/2021/558970 3.

6. Aminuzzaman, M., Kei, L.M., Liang, W.H., 2017. Green synthesis of copper oxide (CuO) nanoparticles using banana peel extract and their photocatalytic activities. AIP Conf. Proc. 1828,. https://doi.org/10.1063/1.4979387 020016.

7. Ashok Kumar, D., Palanichamy, V., Roopan, S.M., 2014. Photocatalytic action of AgCl nanoparticles and its antibacterial activity. J.Photochem. Photobiol. B: Biol. 138, 302–306. https://doi.org/10.1016/j.jphotobiol.20 14.06.011.

8. Baig, U., Uddin, M.K., Gondal, M.A., 2020. Removal of hazardous azo dye from water using synthetic nano adsorbent: Facile synthesis, characterization, adsorption, regeneration and design of

experiments. Colloids Surf. A: Physicochem. Eng. Aspects 584.

9. Balcha, A., Yadav, O.P., Dey, T., 2016. Photocatalytic degradation of methylene blue dye by zinc oxide nanoparticles obtained from precipitation and sol-gel methods. Env. Sci. Poll. Res. 23 (24), 25485–25493. https://doi.org/10.1007/s11356-016-7750-6.

10. Bashiri, M., Rezanezhad, M., Tavakkoli-Moghaddam, R., Hasanzadeh,H., 2018. Mathematical modeling for a p -mobile hub location problem in a dynamic environment by a genetic algorithm. Appl. Math. Mod. 54, 151–169. https://doi.org/10.1016/j.apm.2017.09. 032.

11. Beheshtkhoo, N., Kouhbanani, M.A.J., Savardashtaki, A., Amani, A.M., Taghizadeh, S., 2018. Green synthesis of iron oxide nanoparticles by aqueous leaf extract of Daphne mezereum as a novel dye removing material. Appl. Phy. A. 124 (5). https://doi.org/10.1007/s00339-018-1782-3.Buazar, F., Sweidi, S., Badri, M., Kroushawi, F., 2019. Biofabrication of highly pure copper oxide nanoparticles using wheat seed extract and their catalytic activity: A mechanistic approach. Green Proc. Syn. 8 (1), 691–702. https://doi.org/10.1515/gps-2019-0040.

12. Chavali, M.S., Nikolova, M.P., 2019. Metal oxide nanoparticles and their applications in nanotechnology. SN. Appl. Sci. 1 (6). https://doi.org/10.1007/s42452-019-0592-3.

13. Chemingui, H., Mzali, J.C., Missaoui, T., Konyar, M., Smiri, M.,Yatmaz, H.C., Hafiane, A., 2021a. Characteristics of er-doped zinc oxide layer: Application in synthetic dye solution color removal.

14. Desalin. Water Treat. 209, 402–413. https://doi.org/10.5004/ dwt.2021.26644.

15. Chemingui, H., Missaoui, T., Mzali, J.C., Yildiz, T., Konyar, M.,Smiri, M., Saidi, N.,

Hafiane, A., Yatmaz, H.C., 2019. Facile green synthesis of zinc oxide nanoparticles (ZnO NPs): antibacterial andphotocatalytic activities. Mater. Res. Exp. 6 (10), 1050b4. https://doi.org/10.1088/2053-1591/ab3cd6.

16. Chemingui, H., Rezma, S., Lafi, R., Alhalili, Z., Missaoui, T., Harbi,I., Hafiane, A., 2021b. Investigation of methylene blue adsorption from aqueous solution onto ZnO nanoparticles: equilibrium and Box-Behnken optimisation design. Inter. J. Env. Anal. Chem. 1–26. https://doi.org/10.1080/03067319.2021.1897121.

17. Chung, K.-T., Fulk, G.E., Andrews, A.W., 1978. The mutagenicity of methyl orange and metabolites produced by intestinal anaerobes.Mut. Res. Gen. Tox. 58 (2–3), 375–379. https://doi.org/10.1016/

18. 0165-1218(78)90033-2.

19. Gawande, M.B., Goswami, A., Felpin, F.-X., Asefa, T., Huang, X.,Silva, R., Varma, R.S., 2016. Cu and Cu-Based Nanoparticles:Synthesis and Applications in Catalysis. Chem. Rev. 116 (6), 3722–3811. https://doi.org/10.1021/acs.chemrev.5b00482.

20. Ghaedi, M., Nasab, A.G., Khodadoust, S., Rajabi, M., Azizian, S., 2014. Application of activated carbon as adsorbents for efficient removal of methylene blue: Kinetics and equilibrium study. J. Ind. Eng. Chem. 20 (4), 2317–2324. https://doi.org/10.1016/j.jiec.2013.10.007.

21. Ghasemian, E., Palizban, Z., 2016. Comparisons of azo dye adsorptions onto activated carbon and silicon carbide nanoparticles loaded on activated carbon. Intern. J. Env. Sci. Tech. 13 (2), 501– 512. https://doi.org/10.1007/s13762-015-0875-1.

22. Guey, F., Smiri, M., Chemingui, H., Dekhil, A.B., Elarbaoui, S.,Hafiane, A., 2020. Remove of Humic Acid From Water Using Magnetite Nanoparticles". Eur. J.

Adv. Chem. Res. 1, 1–6. https://doi.org/10.24018/ejchem. 1.4.9.

23. Hekmati, M., 2019. Application of Biosynthesized CuO Nanoparticles Using Rosa canina Fruit Extract as a Recyclable and Heterogeneous Nanocatalyst for Alkyne/Aldehyde/Amine A3 Coupling Reactions. Catal. Let. 149, 2325–2331. https://doi.org/10.1007/s10562-019-02833-4.

24. Ijaz, F., Shahid, S., Khan, S.A., Ahmad, W., Zaman, S., 2017. Green synthesis of copper oxide nanoparticles using Abutilon indicum leaf extract: Antimicrobial, antioxidant and photocatalytic dye degradation activitie. Tropical J. Pharm. Res. 16 (4), 743. https://doi.org/ 10.4314/tjpr.v16i4.2.

25. Iravani, S., 2011. Green synthesis of metal nanoparticles using plants. Green Chem. 13 (10), 2638. https://doi.org/10.1039/c1gc15386b.

26. Jerbi, A., Derbali, A., Elfeki, A., Kammoun, M., 2017. Essential Oil Composition and Biological Activities of Eucalyptus globulus Leaves Extracts from Tunisia. J. Ess. Oil Bear. Plants 20 (2), 438– 448. https://doi.org/10.1080/0972060x.2017.1304832.

27. Kale, R.D., Kane, P.B., 2018. Colour removal of phthalocyanine based reactive dye by nanoparticles. Groundwater Sust. Dev. https://doi.org/10.1016/j.gsd.2018.11.007.

28. Farah, S.D.; Emad, K.; Ali, H. Synthesis Of Selenium Nanoparticles. Eurasian Journal of Physics,Chemistry and Mathematics.2022;7(3):67-71.doi:10.1038/s41598-019-57333-7.

29. Farah S Daabool, Falah H Hussein, Photocatalytic Degradation of Phenol Using TiO^ sub 2^/Active Carbon, Asian Journal of Chemistry,, 282,pp 455,2016. https://cdnx.uobabylon.edu.iq/research/repository1_publication7711_18_2455.pdf

30. Farah S. Daabool And Falah H. Hussein, Synthesis and Characterization of Active

Carbon-Titanium Dioxide Composite, Asian Journal of Chemistry, 31,5,pp1176-1180,2019. https://asianpubs.org/index.php/ajche m/article/view/265/265

31. Farah S. Daabool, Green Synthesis of Nanoparticles Selenium, International Academic Journal of Science and Engineering,Vol. 9, No. 1, 2022, pp. 26-29. https://www.iaiest.com/abstract.php?i d=7&archiveid=1340